Low-Rise Steel Structures under Directional Winds: Mean Recurrence Interval of Failure

D. Duthinh[1]; J. A. Main[2]; A. P. Wright[3]; and E. Simiu[4]

Abstract: The Commentary to the American Society of Civil Engineers (ASCE) Standard 7-05 states that the nominal mean recurrence interval (MRI) of the wind speed inducing the design strength is about 500 years if the specified load factor is 1.5, as in early versions of ASCE 7, and "somewhat higher than 500 years" if the specified load factor is 1.6, as in ASCE 7-05. However, the Commentary also states, "it is not likely that the 500-year event is the actual speed at which engineered structures are expected to fail, due to resistance factors in materials, due to conservative design procedures that do not always analyze all load capacity, and due to a lack of a precise definition of 'failure'." In this paper, we propose a working definition of "failure" for steel structures using nonlinear finite-element analysis, and we present a methodology for estimating the MRI of failure under wind loads that accounts in a detailed and rigorous manner for nonlinear structural behavior and for the directionality of the wind speeds and the aerodynamic effects. The methodology uses databases of wind tunnel pressure (database-assisted design), nonlinear finite-element analysis, and directional wind speeds from the National Institute of Standards and Technology (NIST) hurricane database augmented by statistical techniques. As a case study to illustrate the methodology, we consider a single frame of a steel industrial building. Under the assumption that uncertainties with respect to the parameters that determine the wind loading and to the material behavior are negligible, the minimum MRI of failure for the steel frame being investigated was found to be of the order of 100,000 years, which corresponds to a probability of 1/2,000 that the frame will fail during a 50-year lifetime.

DOI: 10.1061/(ASCE)0733-9445(2008)134:8(1383)

CE Database subject headings: Databases; Failure; Wind direction; Nonlinear analysis; Steel structures; Buildings, low-rise.

Introduction

Section C6.5.4 of the Commentary to ASCE 7-05 (ASCE 2006) defines ultimate wind loads as "loads inducing the design strength . . . " The design strength is typically associated with individual member capacities in tension, bending, and compression. The Commentary further states that the nominal mean recurrence interval (MRI) of the wind loads inducing the design strength is about 500 years if the specified load factor is 1.5, as in early versions of ASCE 7, and "somewhat higher than 500 years" (i.e., about 720 years, according to some wind engineering practitioners) if the specified load factor is 1.6, as in ASCE 7-05. Finally, according to the Commentary, "it is not likely that the 500-year event" (or the 720-year event) "is the actual speed at which engineered structures are expected to fail, due to resistance factors in materials, due to conservative design procedures that do not always analyze all load capacity, and due to a lack of a precise definition of 'failure'." In other words, the Commentary states that we know the 500-year event is not a failure event. On the other hand, we do *not* know the mean recurrence interval of the failure event.

Strictly speaking, owing to a variety of uncertainties with respect to both loading and resistance, in particular uncertainties with respect to the tails of the probability distributions of the extreme wind speeds, that MRI is unknowable, except in notional terms. However, as will be shown in this paper, for certain types of structures, the MRI of the failure event can be estimated with a far higher degree of realism than is possible by using ASCE 7 Standard and related methods. Indeed, the current procedures can account in a detailed and rigorous manner for global nonlinear structural behavior, including load redistribution effects, as well as for directional wind speed and aerodynamic effects. Once MRIs of failure events are estimated, transparent, physically based assessments can be made of actual safety margins inherent in a given design.

In this paper, we present a methodology for estimating the MRI of incipient failure of steel structures under wind loads. The methodology is applied, as a case study, to the analysis of a portal frame belonging to an industrial metal building. Throughout the paper, we assume that uncertainties in the parameters that characterize the wind loading and the material behavior are negligible. We discuss the results in light of the ASCE 7 provisions, and suggest future research aimed at improving standard provisions for wind loads.

[1]Research Structural Engineer, Building and Fire Research Laboratory, National Institute of Standards and Technology, Gaithersburg, MD 20899-8611 (corresponding author). E-mail: dduthinh@nist.gov

[2]Research Structural Engineer, Building and Fire Research Laboratory, National Institute of Standards and Technology, Gaithersburg, MD 20899-8611.

[3]Graduate Student, Dept. of Civil and Environmental Engineering, Carnegie Mellon Univ., Pittsburgh, PA 15213-3890.

[4]NIST Fellow, Building and Fire Research Laboratory, National Institute of Standards and Technology, Gaithersburg, MD 20899-8611.

Note. Associate Editor: Kurtis R. Gurley. Discussion open until January 1, 2009. Separate discussions must be submitted for individual papers. To extend the closing date by one month, a written request must be filed with the ASCE Managing Editor. The manuscript for this paper was submitted for review and possible publication on January 16, 2007; approved on December 27, 2007. This paper is part of the ***Journal of Structural Engineering***, Vol. 134, No. 8, August 1, 2008. ©ASCE, ISSN 0733-9445/2008/8-1383–1388/$25.00.

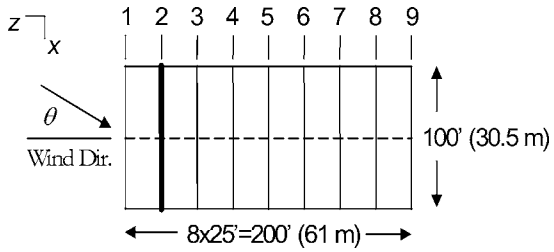

Fig. 1. Plan view of typical frame layout (F1–F9) and wind directions (θ). Location of the selected frame (F2) is in bold and the centerline is shown (- - -).

Overview of Methodology

The methodology entails the following steps:

1. Using database-assisted design software (Main and Fritz 2006; Simiu et al. 2003; Whalen et al. 2000), obtain the load distributions that induce peak internal forces in the structure at a number of cross sections deemed critical. Obtain loads corresponding to a unit wind speed at 10 m above ground over open terrain, and for a number of wind directions θ_i spanning a 360° range. These loads, multiplied by the square of the wind speeds V, are the wind loads considered in the nonlinear analyses in Step 2.
2. Using nonlinear finite-element analysis, determine the wind speed from each direction θ_i that causes the frame to experience incipient failure. The latter is defined as the onset of deformations that increase so fast under load that implicit nonlinear finite-element analysis fails to converge to a solution; it is additionally based on engineering judgment that significant local yielding and buckling have occurred.
3. From available meteorological data, simulate time series of directional wind speeds with a duration (denoted t_d) that exceeds the expected MRI of the failure event.
4. Count the number of failure events n_f produced by the directional wind speed time series from Step 3. The MRI of the failure event for each orientation of interest can then be estimated from the number of failures as $\bar{T}=t_d/n_f$.

This methodology is illustrated in the case study presented next.

Structural Characteristics

The structure analyzed as a case study is a modification of a preliminary design of a low-rise steel warehouse by Ceco Building Systems. The original design was based on ASCE 7-93

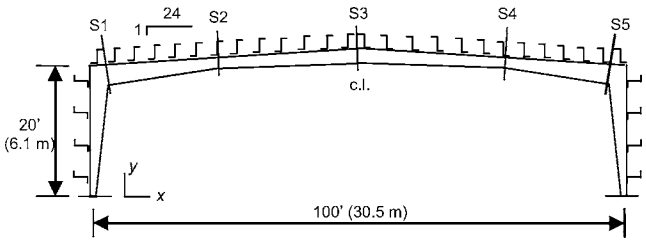

Fig. 2. Schematic of a typical frame at full scale. Moments are calculated at the five sections shown (S1–S5). Structure is symmetric about the centerline (c.l.). Braces below rafters are not shown.

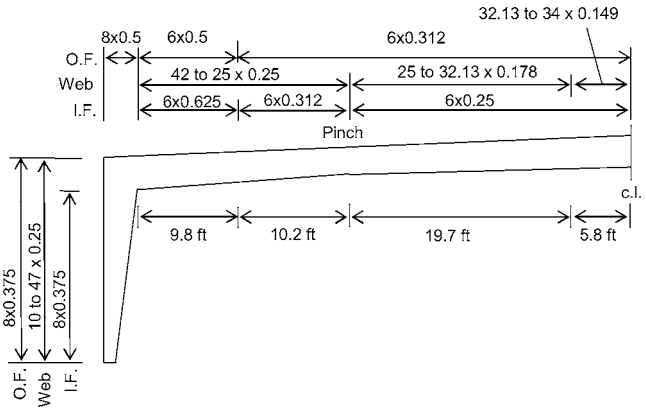

Fig. 3. Typical frame section. Dimensions of outside flange (O.F.), web, and inside flange (I.F.) are given as width (depth) by thickness in inches (1 in.=25.4 mm, 1 ft=304.8 mm)

Standard and allowable stress design (ASD) (AISC 2001), for the coastal region near Miami, Florida. This structure, shown in Figs. 1–3, was studied previously by Jang et al. (2002) and Duthinh and Fritz (2007), who provided a detailed description. The original frame was strengthened in the following manner before analysis:

1. As point supports cause considerable stress concentration, local yielding and distortion, and numerical difficulty at relatively small loads, a base plate and triangular stiffener were added to the frame at each support (Fig. 4), a practical improvement that is recommended for future designs.
2. Another location with high stress concentration is the internal corner between column and rafter (called the haunch). To alleviate this concentration, the frame was modified with the addition of a short oblique member (0.375 in. or 9.5 mm thick) and horizontal, vertical, and diagonal stiffeners that

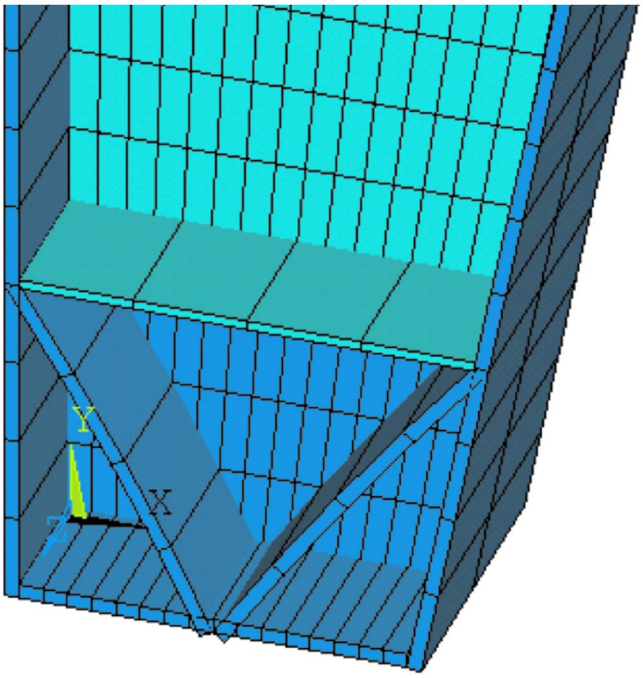

Fig. 4. Base plate and triangular stiffener at support

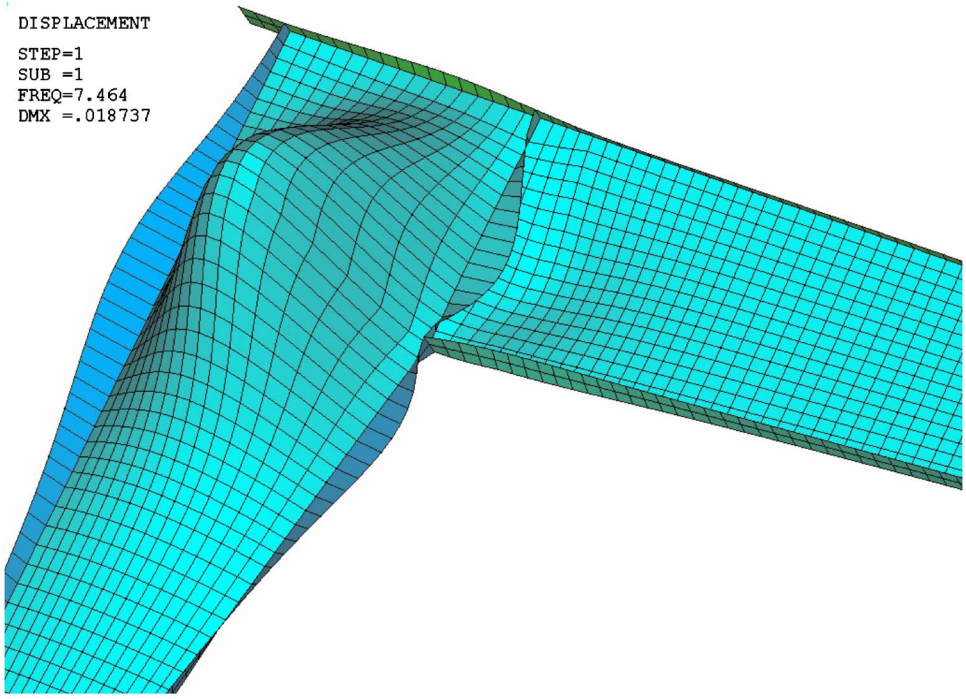

Fig. 5. Initial deformation of left haunch highly exaggerated. Similar initial deformation of right haunch is also used.

allowed an alternative load path at this location. The haunches of the original structure and the modified one are shown in Figs. 5 and 6.

3. In addition, as the governing load cases caused the roof to lift, forcing web and flange local buckling at the ridge (S3, Fig. 2), the modified structure switched the thicker flange from the tension (top) to the compression (bottom) side of the rafter, and kept the web thickness at 0.178 in. (4.5 mm), rather than reducing it to 0.149 in. (3.8 mm) in the ridge region. Finally, web stiffeners were added at the pinches (S2 and S4; Fig. 2).

These structural improvements increased the weight by only 3.6%. Comparison of the performance of the original and the modified structure can be found in Duthinh and Fritz (2007).

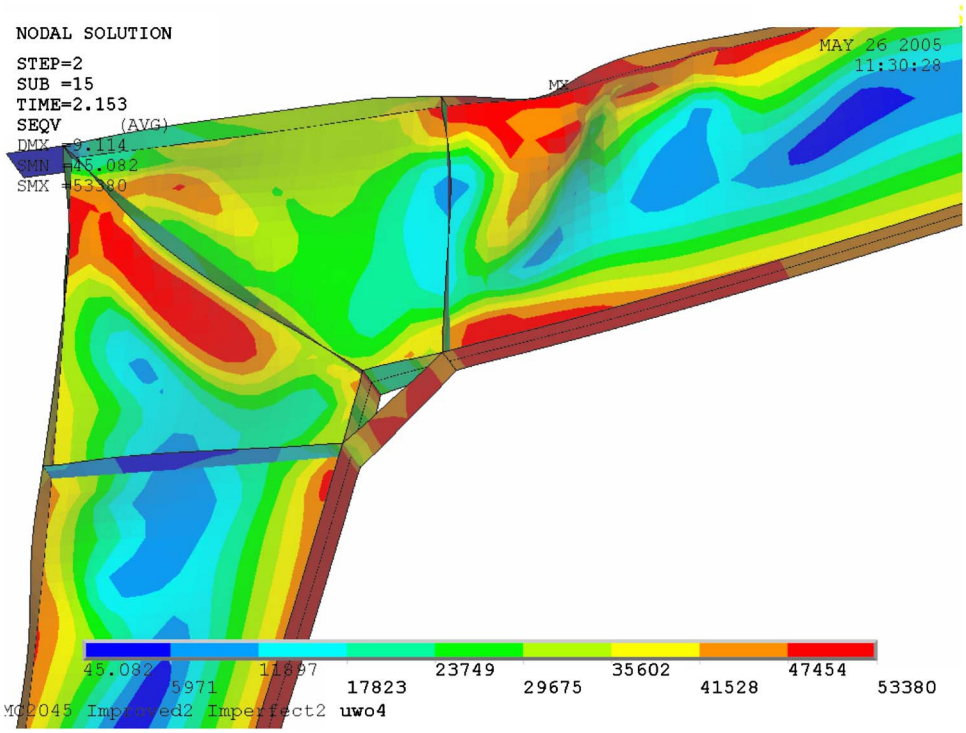

Fig. 6. Left haunch, Von Mises stresses in psi (1 psi=6,895 Pa) at incipient failure

Wind Loads from Wind Tunnel Tests (Step 1)

The wind loads considered in Step 1 of the methodology above were obtained from wind tunnel tests conducted by Ho et al. (2005) on a 1:200 scale model in "open country" terrain conditions. In these tests, pressures at about 550 taps on the model surface were sampled simultaneously at 400 Hz for a duration of 60 s, which corresponds to a full-scale duration of about 1 h. These external pressures were stored in nondimensional form as pressure coefficients C_p, from which the pressure p for a given wind speed V can be obtained as follows:

$$p = \tfrac{1}{2}\rho V^2 C_p \tag{1}$$

where ρ=air density. For consistency with the simulated wind speeds used in Step 4 of the methodology above, the wind speed V in Eq. (1) corresponds to an averaging time of 1 min and an elevation of 33 ft (10 m). To accommodate this definition of V, the original pressure coefficients C'_p, which corresponded to an averaging time of 1 h and an elevation of 20 ft (6.1 m), were rereferenced to obtain the pressure coefficients C_p used in Eq. (1)

$$C_p = \left(\frac{V_{1\ \mathrm{h}}}{V_{1\ \mathrm{min}}}\frac{V_{20\ \mathrm{ft}}}{V_{33\ \mathrm{ft}}}\right)^2 \quad C'_p = \left[\frac{1}{1.25}\left(\frac{20}{33}\right)^{1/7}\right]^2 \quad C'_p \tag{2}$$

where the ratio $V_{1\ \mathrm{min}}/V_{1\ \mathrm{h}}=1.25$ follows from Fig. C6-2 of ASCE 7-05 and the ratio $V_{20\ \mathrm{ft}}/V_{33\ \mathrm{ft}}=(20/33)^{1/7}$ follows from a power-law approximation of the mean velocity profile for "open country" terrain (Simiu and Scanlan 1996; Simiu and Miyata 2006).

Wind tunnel tests were conducted over a 180° range of the wind direction θ (see Fig. 1), and symmetry of the wind tunnel model was exploited to extend these measurements over a 360° range, as described in Main and Fritz (2006). In the present analysis, pressure time series for 36 wind directions $\theta_i=10°(i-1)$, $i=1,\ldots,36$ were considered, spanning a 360° range in 10° increments. These pressure time series were transformed to time series of resultant loads on the selected structural frame as described in Main and Fritz (2006). Pressures corresponding to a unit wind speed V were considered, so that resultant structural loads for any wind speed of interest can be obtained through scaling by V^2, according to Eq. (1). In addition to the external wind loads obtained from wind tunnel tests, loads resulting from the internal pressures recommended by ASCE 7-05 for enclosed buildings were also considered.

To determine worst-case load distributions for use in the nonlinear finite-element analysis of Step 2, five cross sections in the structural frame were selected for consideration, labeled S1 through S5 in Fig. 2. For each wind direction θ_i, the largest positive and negative bending moments at each cross section were computed from the time series of resultant structural loads, and the instantaneous structural loads corresponding to each peak were saved, yielding 10 load cases for each direction θ_i. The bending moments were computed using a linear, static structural model consisting of frame elements with pinned column bases and compared with the moment capacity of the sections of interest. The moment capacities were assumed to cause yielding or elastic buckling of the flanges or web. The selection of the most critical load cases made use of this comparison and also of symmetry and similarity between wind pressure distributions corresponding to various load cases. The internal and external wind loads, multiplied by the square of the wind speed V, were considered in the detailed, nonlinear finite-element analysis described in the following section. The results of the nonlinear analyses were verified to ensure that the assumptions used in load case selection were respected, i.e., the governing critical sections occurred where predicted. Based on the results of the linear analysis, wind pressures causing maximum bending moment at section S1 were selected for further nonlinear analysis for wind directions spanning from 0 to 180° in 10° increments. In addition and for a few directions, wind pressures causing maximum bending moment at section S3 were also analyzed nonlinearly to confirm that they did not govern.

Nonlinear Finite-Element Analysis (Step 2)

The finite-element model used 11,000 shell elements, the great majority of which have a typical dimension of 3 in. (76 mm). The element used has four corner nodes with six degrees of freedom each. The model is three dimensional in the sense that all six degrees of freedom are considered, but since only one frame is analyzed, the purlins, girts, and braces are modeled as constraints to resist out-of-plane translation. The material used in the model was steel, with a modulus of elasticity of 29,000 ksi (200 GPa), a yield strength of $\sigma_y=50$ ksi (344 MPa), an ultimate strength of $\sigma_u=65$ ksi (448 MPa), and a gradual stress-strain curve beyond yield, similar to the actual design material.

In a first load step, gravity was applied with a factor of 0.9, and the structure analyzed. In the second step, wind load was applied in incremental fashion until the structure failed. The criterion for incipient failure is excessive element distortion resulting in the implicit structural analysis program being unable to converge to a solution, even after repeated halving of load increments. Numerical divergence had to correspond to actual physical imminent collapse as seen from significant local buckling and/or section yielding before attempts at restarting the program were abandoned.

Since local buckling played an important role in the ultimate strength of the structure, the analysis accounted for initial imperfections. For local plate buckling, the relevant dimensions are width and thickness, not length. Most plates in the frame have a width to thickness ratio of about 200, and a rather severe, initial out-of-plane deformation amplitude of 1% of width, or 0.3 in. (7.6 mm) was selected (Fig. 5). Initial deformations were obtained from linear combinations of (linear) eigenvalue buckling modes selected to occur at critical sections S1–S5.

A typical graphical output from the nonlinear analysis of Step 2 (Fig. 6) shows large deflections, considerable local buckling, and partial yielding of the cross section. Other parts of the structure are similarly stressed, almost to the point of formation of plastic hinges and failure mechanisms. From the nonlinear finite-element analysis, the wind speed at failure is obtained. Fig. 7 shows a plot of the resulting failure wind speeds versus wind direction θ. The minimum failure speed was found to be 152 knots (78.2 m/s), corresponding to wind directions of $\theta=40°$ and $\theta=320°$.

Simulation of Directional Wind Speeds (Step 3)

Step 3 of the methodology above requires directional wind speeds at the location of interest spanning a duration t_d that exceeds the expected MRI of the failure event. Simulated directional hurricane wind speeds for Miami are available at the site, http://www.nist.gov/wind, for 16 different wind directions $\phi_j=22.5°j$, where $j=1,\ldots,16$, measured in degrees clockwise

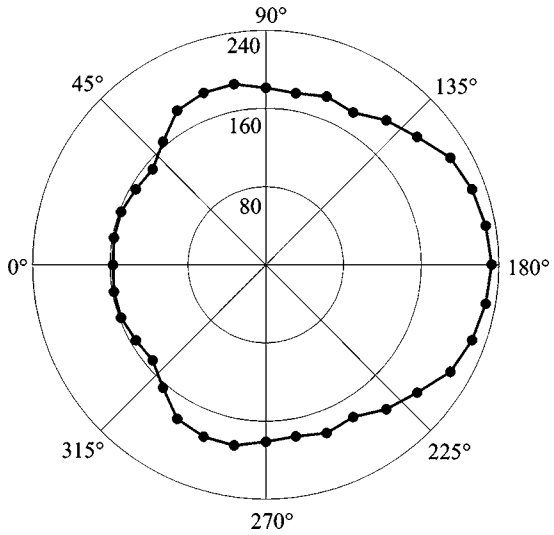

Fig. 7. Failure wind speed (in knots) versus wind direction (1 knot =0.5144 m/s)

from true north. However, these data span a period of 1,780 years (999 storms with a mean arrival rate of 0.56/year), which is not sufficiently long. Therefore, these data were augmented through Monte Carlo simulation to span a duration of t_d=200,000 years (112,022 storms). Clearly, the simulation of wind speeds over such a long period of time entails considerable uncertainties, especially given that the original 999 storms were simulated on the basis of historical data from a much shorter time.

The directional wind speed simulations used a procedure developed by Grigoriu (2006a,b), and Grigoriu's reports are available at the website, www.nist.gov/wind, along with MATLAB implementations of the simulation procedure. While Grigoriu presents a procedure to account for correlations between wind speeds from different directions, estimation of the requisite correlation matrix poses difficulties because a significant fraction of the directional wind speed values in the original data set are zero (i.e., in a given hurricane, nonzero wind speeds were only recorded from certain wind directions, and the wind speeds from other directions were assigned zeros). Because of these difficulties, Grigoriu (2006a) recommends simulations that assume statistical independence among the wind speeds from different directions, and the simulations used in this study are based on this assumption.

To represent the finite probability of occurrence of zero values, the wind speed from a given direction ϕ_j is represented as a generalized Bernoulli variable that (1) is zero with probability $1-p_j$ and (2) is a reverse Weibull random variable with probability p_j. The probability p_j for wind direction ϕ_j is estimated as the fraction of nonzero wind speeds from that direction in the original data set. The reverse Weibull cumulative distribution function for the wind speeds of v from direction ϕ_j can be expressed as follows:

$$F_j(v) = \exp\left[-\left(\frac{\eta_j - v}{\alpha_j}\right)^{c_j}\right] \tag{3}$$

The distribution parameters η_j, α_j, and c_j for wind direction ϕ_j are estimated from the mean, variance, and skewness, respectively, of the *nonzero* wind speed values from that wind direction, using the method of moments. A maximum permissible value of c_j=10 was imposed to avoid unrealistic estimates of the shape parameter.

Table 1. Simulated Hurricane Wind Speeds and Directions for Storms in Which the Minimum Failure Wind Speed of 152 Knots Is Exceeded (1 Knot=0.5144 m/s)

Storm	Wind speed (knots)	Wind direction, ϕ (° clockwise from north)
43,883	161	22.5
73,212	153	247.5
92,464	192	247.5
97,844	155	270
102,570	182	22.5
102,950	153	225

Once the probabilities p_j and the reverse Weibull parameters η_j, α_j, and c_j for each wind direction have been estimated from the original data set, directional wind speeds can be simulated using a translation model. The resulting directional wind speed time series can be represented as a matrix $\mathbf{V}$, in which the rows correspond to samples in time and the columns correspond to the 16 wind directions ϕ_j. The elements of $\mathbf{V}$ are obtained by first generating a matrix $\mathbf{U}$, of the same size as $\mathbf{V}$, whose elements are statistically independent random numbers from a uniform distribution on the interval (0,1). For each element U_{ij} of $\mathbf{U}$, if $U_{ij}<1-p_i$, then the corresponding element V_{ij} of $\mathbf{V}$ is assigned a zero value. If $U_{ij}\geq 1-p_i$, then a cumulative probability of $\tilde{U}_{ij}=[U_{ij}-(1-p_i)]/p_i$ is calculated for the reverse Weibull distribution, and the wind speed V_{ij} is estimated from the inverse of the reverse Weibull distribution as $V_{ij}=F_j^{-1}(\tilde{U}_{ij})$. Using this procedure, the matrix $\mathbf{V}$ of directional wind speeds can be extended to span the required duration t_d.

MRI of Failure (Step 4)

In Step 4 of the methodology above, the directional wind speeds in the matrix $\mathbf{V}$ are compared with the failure wind speeds from Step 2 to determine the number of failures that result for different building orientations, along with the corresponding MRIs of failure. The number of failures n_f is given by the number of rows in $\mathbf{V}$ for which the failure wind speeds from Step 2 are exceeded in at least one direction. Note that n_f depends on building orientation, because the wind directions ϕ_j must be shifted by the building orientation ϕ_0 for consistency with the wind directions θ_i for which failure wind speeds were evaluated in Step 2. The symbol $\hat{\theta}_j=\phi_j-\phi_0$ is introduced to denote these shifted wind directions. Because the values of $\hat{\theta}_j$ generally do not coincide with the values of θ_i (e.g., in this case there is an increment of 10° between the values of θ_i but an increment of 22.5° between the values of $\hat{\theta}_j$), a sector-based approach for assessing failure is adopted. Let $\Delta\hat{\theta}_j$ denote the sector corresponding to $\hat{\theta}_j$, which is bounded above by the midpoint between $\hat{\theta}_j$ and $\hat{\theta}_{j+1}$, and bounded below by the midpoint between $\hat{\theta}_j$ and $\hat{\theta}_{j-1}$, with both bounds inclusive. A wind speed reported for direction $\hat{\theta}_j$ could potentially correspond to any wind direction within the sector $\Delta\hat{\theta}_j$, and, therefore, failure is assumed to occur if the failure wind speed is exceeded for any wind direction θ_i within the sector $\Delta\hat{\theta}_j$.

Examination of the simulated wind speed data for Miami revealed that the minimum failure speed of 152 knots (78.2 m/s) was exceeded in only six of the 112,022 simulated storms, and the directional wind speeds for these storms are shown in Table 1. As

Table 2. Estimated Number of Failures n_f and Corresponding MRIs $\bar{T}$ (Years) for Different Building Orientations

Building orientation, ϕ_o	n_f	$\bar{T}$ (years)
0°, 22.5°	3	66,700
45°, 67.5°	2	100,000
90°	1	200,000
112.5°, 135°, 157.5°, 180°	2	100,000
202.5°, 225°	3	66,700
247.5°, 270°, 292.5°	4	50,000
315°,337.5°	3	66,700

in Fig. 7, these wind speeds correspond to an averaging time of 1 min at an elevation of 33 ft (10 m) over open terrain. The directional wind speeds in Table 1 were then compared with the failure wind speeds in Fig. 7 for 16 different building orientations, and the results are shown in Table 2. While the computed MRIs of failure seem quite high, it is noted that an MRI of the order of 100,000 years corresponds to a probability of 1/2,000 that the frame will fail during a 50-year lifetime. Given that this frame incorporates additional stiffeners to improve its strength, this figure does not seem unreasonable. It is also noted that the methodology outlined in this paper does not account for variability in structural resistance, and, thus, the MRI estimates in this paper must be considered approximations. A methodology that accounts for such variability in the estimation of failure MRIs is currently in development.

Conclusion

This paper presents a methodology for estimating the mean recurrence interval (MRI) of failure under wind loads that accounts for nonlinear structural behavior and the directionality of the wind speeds and the aerodynamic effects, and uses databases of wind tunnel test results as well as wind speed data from the NIST hurricane wind speed database augmented by statistical methods. Under the assumption that uncertainties with respect to the parameters governing wind loading and material performance are negligible, our methodology results in a notional probability of failure during a 50-year period of the order of 1/2,000. This result was obtained for one particular low-rise steel structure at one particular location, but the method is general and can be applied to any structure anywhere provided the relevant meteorological and wind tunnel data exist and nonlinear finite-element analysis is accessible. As different structures fail by different mechanisms, good engineering judgment is required to identify potential critical load cases and to limit nonlinear analysis to a manageable number of cases.

Our results can be compared with the estimate of the probability of exceedance of the limit state consisting of the first attainment of the yield stress in the structure designed in accordance with the ASCE 7 Standard. That probability is, notionally, about 1/500 per year, or $1-0.998^{50}=0.1$ during a 50-year lifetime. (We note that the probability of exceedance of this limit state should be expected to be lower for our structural frame, which has been strengthened beyond the initial ASCE 7 design.) The probabilities of failure presented in this paper are more rigorous in two respects. First, they account for the postfirst-yield capacity of the structure. Second, they account more faithfully for the wind climatology, building aerodynamics, and their joint dependence on direction. Through this more rigorous physical basis, our results allow meaningful comparisons to be made on the basis of the respective failure probabilities between various designs. Once a professional consensus is reached on appropriate models to be used in a procedure similar to ours, a methodology will have been developed that would make it possible to assess designs on the basis of such notional failure probabilities as that analysis would yield.

Disclaimer

Certain trade names or company products are mentioned in the text to specify adequately the experimental procedure and software used. In no case does such identification imply recommendation or endorsement by the National Institute of Standards and Technology (NIST), nor does it imply that the equipment or software is the best available for the purpose. The policy of the NIST is to use the International System of Units (SI or metric units) in all its publications. However, in the United States, in the construction and building materials industry, certain non-SI units are so widely used instead of SI units that it is more practical and less confusing to include customary units as the principal units of measurements.

References

American Institute of Steel Construction (AISC). (2001). *Load and resistance factor design specification for structural steel buildings*, 3rd Ed., Chicago.

American Society of Civil Engineers (ASCE). (2006). "Minimum design loads for buildings and other structures." *SEI/ASCE7-05*, Reston, Va.

Duthinh, D., and Fritz, W. P. (2007). "Safety evaluation of low-rise steel structures under wind loads by nonlinear database-assisted technique." *J. Struct. Eng.*, 133(4), 587–594.

Grigoriu, M. (2006a). "A model for directional hurricane wind speeds." *NIST Government Contractor Rep. No. GCR 06-905*, Gaithersburg, Md., ⟨http://www.itl.nist.gov/div898/winds/pdf_files/GCR06-905.pdf⟩.

Grigoriu, M. (2006b). "Probabilistic models for directionless wind speeds in hurricanes." *NIST Government Contractor Rep. No. GCR 06-906*, Gaithersburg, Md., ⟨http://www.itl.nist.gov/div898/winds/pdf_files/GCR06-906.pdf⟩.

Ho, T. C. E., Surry, D., Morrish, D., and Kopp, G. A. (2005). "The UWO contribution to the NIST aerodynamic database for wind loads on low buildings: Part 1. Archiving format and basic aerodynamic data." *J. Wind. Eng. Ind. Aerodyn.*, 93(1), 1–30.

Jang, S., Lu, L. W., Sadek, F., and Simiu, E. (2002). "Database-assisted wind load capacity estimates for low-rise steel frames." *J. Struct. Eng.*, 128(12), 1594–1603.

Main, J. A., and Fritz, W. P. (2006). "Database-assisted design for wind: Concepts, software, and examples for rigid and flexible buildings." *NIST Building Science Series 180*, Gaithersburg, Md.

Simiu, E., et al. (2003). "Achieving safer and more economical buildings through database-assisted, reliability-based design for wind." *J. Wind. Eng. Ind. Aerodyn.*, 91(12–15), 1587–1611.

Simiu, E., and Miyata, T. (2006). *Design of buildings and bridges for wind*, Wiley, Hoboken, N.J.

Simiu, E., and Scanlan, R. H. (1996). *Wind effects on structures*, 3rd Ed., Wiley, New York.

Whalen, T., Shah, V., and Yang, J. S. (2000). "A pilot project for computer-based design of low-rise buildings for wind loads—The WILDE-LRS user's manual." *NIST Government Contractor Rep. No. GCR 00-802*, Gaithersburg, Md.